

The behaviour of Mn in amphiboles : Mn in richterite

ROBERTA OBERTI, FRANK C. HAWTHORNE *, LUCIANO UNGARETTI
and ELIO CANNILLO

CNR, Centro di Studio per la Cristallografia e la Cristallografia
via A. Bassi 4, I-27100 Pavia, Italy

Abstract : The crystal structures and site occupancies of 5 manganous richterites have been refined to R indices $\leq 2\%$ using single-crystal MoK α X-ray diffraction data. For all these amphiboles, EMP analyses indicate significant occupancy of the M(4) site by (Mn²⁺, Fe²⁺, Mg). Difference-Fourier maps show the presence of electron density within the M(4) cavity but displaced along the 2-fold axis towards the octahedral strip ; this position is designated M(4'). The local stereochemistry about the M(4') site is very similar to that around the M(4) site in the monoclinic ferromagnesian amphiboles, suggesting that the M(4') site is occupied by (Mn²⁺, Fe²⁺, Mg). Comparison between the results of the structure refinements and of EMP analyses of the same richterite crystals indicate that the M(4') site is dominantly occupied by Mn²⁺. At the octahedrally-coordinated M(1,2,3) sites, Mn is present as Mn²⁺ and is strongly ordered at the M(2) site.

The <M(1)-O> and <M(3)-O> distances in richterites are linear functions of the amount of F⁻ \rightleftharpoons OH⁻ substitution at the O(3) site. The need for dimensional matching among the three independent octahedral sites suggests that extensive F⁻ substitution is inhibited in manganous richterites, in which the M(2) site is particularly large.

Keywords : manganese, richterite, crystal-chemistry, amphibole.

1. Introduction

The behaviour of manganese in amphiboles is not very well known. In most types of amphiboles, this is not a problem as Mn is only a minor or a trace constituent. However, in some amphiboles from Mn-rich parageneses, Mn can be a major constituent, and its crystal-chemical behaviour is then of importance. The problem is further complicated by the fact that Mn can occur in two valence states in amphiboles : Mn²⁺ and Mn³⁺. Most quantitative information on the behaviour of specific cation species in amphiboles is derived from X-ray scattering experiments via crystal-structure refinement. The problem of adequately characterizing the distribution of Mn is in general fairly intractable for two reasons:

- (1) the X-ray scattering factors of Mn²⁺ and Mn³⁺ are practically indistinguishable from those of Fe²⁺ and Fe³⁺ ;
- (2) environments rich in Mn are also usually rich in Fe because of the geochemical coherence of these two species, and therefore manganiferous amphiboles are usually Fe-rich. The problem of distinguishing Mn from Fe is in principle susceptible to solution using neutron diffraction, as the scattering lengths of Fe and Mn are very different (Bacon, 1969). The additional complication given by the presence of other scatterers (specifically Mg) occupying the same sites can be circumvented by doing both X-ray and neutron structure refinements (Hawthorne, 1983a). However, this rather complicated procedure cannot be considered as a general solution, because of the

* Permanent address : Department of Geological Sciences, University of Manitoba, Winnipeg, Manitoba, Canada R3T 2N2

scarce availability of neutron sources and the stringent (large) size requirements for crystals used in neutron diffraction experiments.

On the other hand, when significant amounts of Mn are present, the crystal-chemical analysis of the results of the structure refinements can rely also on mean bond lengths and standard stereochemical relationships (Ungaretti, 1980 ; Hawthorne, 1983b). They should in principle allow one to assign Mn at the differing structural sites, and to discriminate between Mn²⁺ and Mn³⁺. This has been done in the case of two Mn³⁺-bearing amphiboles by Ghose *et al.* (1986). The complexity of the chemical composition of amphiboles, in which up to seven cations (Mg, Al, Mn²⁺, Mn³⁺, Fe²⁺, Fe³⁺, Ti⁴⁺) can be present simultaneously at the octahedral sites, often precludes this possibility.

We have chosen to approach this problem by examining specific amphiboles in which the compositional problems hindering a solution are reduced to a minimum. Moreover, we have chosen to start with amphibole end-members for which a good knowledge of the crystal-chemical behaviour of the other constituent cations is available, in order to exploit this kind of information in comparative crystal-chemical work. In this first paper, we examine the behaviour of Mn in richterites. The following contractions are used : m.a.n. = mean atomic number ; m.b.l. = mean bond length ; a.p.f.u. = atoms per formula unit ; e.s.d. = estimated standard deviation.

2. Experimental

Two rock-samples containing manganoan richterites with different Mn contents were examined in this work. They both come from Långban, Sweden ; one was kindly supplied by M. Bondi (University of Bologna, Italy) [MR(1-3)] and the other is from the collection of the Department of Earth Science, University of Pavia [MR(4-5) ; sample # 9740].

2.1 X-ray data collection

The crystals used in this work were selected on the basis of optical behaviour and freedom from inclusions, mounted on a Philips PW 1100 automated four-circle diffractometer and examined with graphite-monochromated Mo-K α -X-radiation ; crystal quality was assessed *via* the profiles and widths of Bragg diffraction peaks.

Table 1. Unit-cell dimensions and miscellaneous structure refinement information for richterites ; maximum e.s.d. in unit-cell dimensions are < 2 on the last figure.

	MR(1)	MR(2)	MR(3)	MR(4)	MR(5)
a (Å)	9.891	9.892	9.909	9.966	9.974
b (Å)	18.018	18.027	18.030	18.066	18.078
c (Å)	5.276	5.278	5.278	5.279	5.282
β (°)	104.15	104.09	104.23	104.40	104.36
V (Å ³)	911.76	912.95	914.05	920.58	922.67
θ_{max} (°)	30	35	32	35	53
D _c	3.10	3.09	3.09	3.09	3.09
# _{hkl}	1383	2087	1661	2106	5504
# _{obs} >5 σ (I)	954	1429	1340	1626	3545
R _{sym}	2.3	1.6	1.6	2.4	2.4
R _{obs}	1.5	1.4	1.4	1.6	2.0
R _{int}	2.9	3.0	2.1	2.5	4.3

Unit-cell dimensions were calculated from least-squares refinement of the *d* values obtained for 48 rows of the reciprocal lattice by measuring the center of gravity of each reflection (1 to 4 in each row) in the θ range 2-35°, together with that obtained for the same reflection at negative θ values. Unit-cell dimensions for the crystals used in the X-ray data collection are given in Table 1 ; their e.s.d.'s are approximately equal to 2 on the last digit.

Intensity data were collected for the monoclinic-equivalent pairs *hkl* and *h \bar{k} l* in the Laue group 2/*m* in the θ range 2-(30-35)° using the step-scan profile technique of Lehman and Larsen (1974). For sample MR(5) a high-resolution data collection up to $\theta = 53^\circ$ was performed. Full details of the data collection procedure are given in Ungaretti (1980) and Ungaretti *et al.* (1981). The intensity data were corrected for Lorentz and polarization effects and for absorption by the method of North *et al.* (1968), merged and reduced to structure factors. A reflection was considered as observed if its intensity exceeds that of five standard deviations.

2.2 Structure refinement (XRef)

Fully ionized scattering factors were used for non-tetrahedral cations, whereas both neutral and ionized scattering factors were used for the tetrahedral cations and the oxygens (Ungaretti, 1980). In the case of the tetrahedral T(1) sites, a mixed scattering curve corresponding to Si_{0.95}Al_{0.05} was used for MR(1-3), based on the results of the EMP analyses. This model was found to be in agreement with observed <T(1)-O> distances. All the atomic positions but H and M4' were refined using anisotropic thermal factors.

For all the samples, the equivalent isotropic displacement parameters obtained at convergence for the O(3) oxygens were systematically and significantly lower than those obtained for the other oxygens and for the O(3) site in other OH-amphiboles, suggesting the presence of partial F⁻ substitution for hydroxyl. At the O(3) site, the scattering factor of O⁻ was therefore used against that of F⁻ in the last cycles of the structure refinement.

Difference-Fourier maps obtained at convergence for all the samples showed the presence of significant residual electron density near to the M(4) site, but displaced along the 2-fold axis towards the octahedral strip; this position had been called M(4') by Ungaretti *et al.* (1981). These peaks of residual electron density have an *y* coordinate similar to that obtained by Papike *et al.* (1969) in the refinement of a manganooan cummingtonite with 1.58 Mn²⁺ a.p.f.u. at the M(4) site. Accordingly, the scattering curve for Mn²⁺ was used to refine the occupancy of this split site in the subsequent cycles of the refinement (see Section 3.3 for a more detailed discussion and Rossi *et al.* (1987) for technical details of the refinement in the analogous case of the M(2') site in clinopyroxenes). It should be noted here that the refined occupancy of the M(4') site is not very reliable, as the refinement procedure is operating at the limits of its resolution. The separation of the M(4) and M(4') sites is less than 0.40 Å, approximately half the wavelength of the scattered radiation; hence the two sites cannot be refined reliably as independent sites. However, the sum of the occupancy at the M(4)+M(4') sites is an accurate measure of the aggregate scattering at these sites.

Concerning the A cations, the split A-site model (Hawthorne, 1983b) was used in the refinement. It consists of the special position A(2/*m*), with coordinates 0,1/2,0, and of the two split positions A(*m*), with coordinates *x*,1/2,*z*, and A(2), with coordinates 0,*y*,0. Also in this case, the three sites cannot be refined independently. However, the sum of the occupancies at A(2/*m*), A(*m*) and A(2) has proven to be an accurate measurement of the m.a.n. at the A site (Ungaretti *et al.*, 1981).

All the refinements were done in the space group C2/*m*, and converged to conventional *R* factors ≤ 2% (Table 1) for the observed reflections. Atomic coordinates and equivalent isotropic displacement parameters are given in

Table 2. Atomic fractional coordinates ($\times 10^4$) and equivalent isotropic displacement parameters (\AA^2); e.s.d. < 1 on the last figure.

		MR(1)	MR(2)	MR(3)	MR(4)	MR(5)	
0(1)	<i>x/a</i>	1120	1119	1115	1117	1117	
	<i>y/b</i>	857	858	858	854	854	
	<i>z/c</i>	2170	2168	2171	2181	2179	
	B	0.58	0.55	0.55	0.61	0.58	
0(2)	<i>x/a</i>	1198	1198	1197	1195	1195	
	<i>y/b</i>	1701	1701	1702	1697	1697	
	<i>z/c</i>	7249	7244	7247	7235	7230	
	B	0.66	0.64	0.63	0.69	0.67	
0(3)	<i>x/a</i>	1072	1074	1071	1066	1066	
	<i>z/c</i>	7136	7135	7138	7147	7149	
	B	0.77	0.69	0.69	0.76	0.69	
0(4)	<i>x/a</i>	3639	3638	3638	3621	3622	
	<i>y/b</i>	2476	2477	2476	2471	2470	
	<i>z/c</i>	7897	7903	7904	7927	7925	
	B	1.01	1.00	0.96	0.94	0.93	
0(5)	<i>x/a</i>	3465	3464	3462	3445	3443	
	<i>y/b</i>	1307	1307	1311	1301	1301	
	<i>z/c</i>	885	885	906	898	897	
	B	0.89	0.87	0.85	0.81	0.80	
0(6)	<i>x/a</i>	3425	3426	3425	3416	3414	
	<i>y/b</i>	1161	1162	1160	1163	1164	
	<i>z/c</i>	5876	5877	5898	5889	5888	
	B	0.92	0.88	0.85	0.83	0.82	
0(7)	<i>x/a</i>	3379	3378	3376	3358	3357	
	<i>z/c</i>	2854	2858	2860	2911	2914	
	B	1.01	0.97	0.94	0.95	0.91	
	T(1)	<i>x/a</i>	2789	2789	2786	2774	2773
<i>y/b</i>		847	847	847	845	845	
<i>z/c</i>		2932	2932	2944	2950	2949	
B		0.49	0.43	0.42	0.47	0.42	
T(2)	<i>x/a</i>	2877	2876	2874	2860	2860	
	<i>y/b</i>	1709	1709	1709	1707	1707	
	<i>z/c</i>	7992	7991	8002	8001	8000	
	B	0.50	0.48	0.46	0.49	0.45	
M(1)	<i>y/b</i>	888	887	888	888	888	
	B	0.58	0.54	0.52	0.56	0.51	
M(2)	<i>y/b</i>	1800	1800	1798	1806	1807	
	B	0.61	0.61	0.61	0.64	0.60	
M(3)	B	0.55	0.50	0.50	0.54	0.49	
	M(4)	<i>y/b</i>	2742	2752	2756	2768	2769
B		1.30	1.15	1.14	0.99	0.94	
M(4')	<i>y/b</i>	2509	2578	2558	2604	2578	
	B	0.32	0.84	0.89	1.24	0.98	
	A(2/ <i>m</i>)	B	3.58	3.96	2.84	3.81	3.76
		A(<i>m</i>)	<i>x/a</i>	368	378	351	272
<i>z/c</i>	876		885	856	763	816	
A(2)	B	3.53	3.60	2.77	4.93	4.57	
	<i>y/b</i>	4646	4654	4666	4679	4711	
	B	2.06	3.45	2.90	1.86	2.16	
	H	<i>x/a</i>	1938	1904	1836	1881	1939
<i>z/c</i>		7807	7461	7468	7640	7591	
B		1.35	0.64	3.10	2.11	2.18	

Table 2; selected interatomic distances are given in Table 3, and the mean atomic numbers for the structural sites are listed in Table 4. Tables of observed and calculated structure factors and anisotropic displacement parameters may be obtained on request from the authors or through E.J.M. Editorial Office.

2.3 Electron microprobe analysis

The same grains used in the X-ray data collection were later analyzed by the electron micro-

Table 3. Individual and mean bond distances (Å) in richterites; e.s.d. are < 1 on the last figure.

	MR(1)	MR(2)	MR(3)	MR(4)	MR(5)
T(1)-0(1)	1.601	1.603	1.605	1.599	1.600
-0(5)	1.629	1.629	1.631	1.631	1.631
-0(6)	1.628	1.631	1.633	1.629	1.630
-0(7)	1.638	1.638	1.639	1.636	1.637
<T(1)-0>	1.624	1.625	1.625	1.626	1.624
T(2)-0(2)	1.610	1.611	1.611	1.608	1.609
-0(4)	1.582	1.582	1.582	1.579	1.581
-0(5)	1.660	1.662	1.663	1.665	1.666
-0(6)	1.677	1.676	1.676	1.680	1.679
<T(2)-0>	1.632	1.633	1.633	1.633	1.634
M(1)-0(1)	2.066	2.066	2.065	2.069	2.071
-0(2)	2.067	2.068	2.069	2.061	2.063
-0(3)	2.090	2.091	2.091	2.094	2.097
<M(1)-0>	2.075	2.075	2.075	2.075	2.077
M(2)-0(1)	2.192	2.192	2.187	2.211	2.213
-0(2)	2.094	2.096	2.097	2.110	2.113
-0(4)	2.003	2.003	2.006	2.011	2.012
<M(2)-0>	2.096	2.097	2.097	2.111	2.113
M(3)-0(1) x2	2.074	2.076	2.075	2.076	2.077
-0(3)	2.047	2.049	2.048	2.048	2.047
<M(3)-0>	2.065	2.067	2.066	2.066	2.067
M(4)-0(2)	2.377	2.391	2.394	2.420	2.421
-0(4)	2.304	2.310	2.316	2.349	2.348
-0(5)	2.887	2.880	2.863	2.872	2.876
-0(6)	2.625	2.612	2.616	2.609	2.611
<M(4)-0>	2.548	2.548	2.547	2.563	2.564
M(4')-0(2)	2.061	2.150	2.122	2.190	2.156
-0(4)	2.270	2.275	2.279	2.313	2.310
-0(5)	3.155	3.076	3.087	3.055	3.090
-0(6)	2.955	2.855	2.893	2.835	2.875
<A(2/m)-0>	2.908	2.910	2.913	2.928	2.932
<A(m)-0>	2.844	2.845	2.852	2.872	2.869
<A(2)-0>	2.569	2.576	2.586	2.615	2.638
H-0(3)	0.843	0.797	0.736	0.789	0.844

probe (EMP). The crystals were mounted in piccolite in small holes in one-inch perspex discs; each disc also contained several crystals of tremolite (56) of Hawthorne (1983b) to check for analytical accuracy and mount-to-mount compatibility. The discs were polished and carbon-coated.

Electron microprobe analyses were done on a fully-automated Cameca SX-50 operating in the wavelength-dispersive mode with the following conditions: excitation voltage: 15 kV; specimen current: 20 nA; peak count time: 20 s; background count time: 10 s. The following standards and crystals were used for K α X-ray lines:

Table 4. Refined mean atomic numbers (electrons) in richterites; e.s.d. are ~ 0.1 electrons.

	MR(1)	MR(2)	MR(3)	MR(4)	MR(5)
M(1)	12.8	12.7	12.8	13.1	13.1
M(2)	16.2	16.2	16.1	17.9	18.1
M(3)	12.4	12.3	12.5	12.6	12.6
M(4)	16.2	15.1	15.8	15.1	15.1
M(4')	0.7	1.7	1.2	0.8	0.8
A(2/m)	5.0	5.4	4.9	7.0	7.5
A(m)	2.5	2.2	2.5	2.2	1.9
A(2)	0.7	1.1	1.2	0.7	0.8
O(3)	8.3	8.3	8.3	8.3	8.2

Al: Al₂O₃, TAP; Fe: fayalite, LiF; Si: diopside, PET; Mg: MgO, TAP; F: fluor-riebeckite, TAP; Mn: tephroite, LiF; Ti: titanite, LiF. Each grain was analysed at a minimum of 10 points (commonly twice this number, depending on the size of the exposed surface) to check for compositional zoning and to obtain a representative composition for the whole crystal used in the collection of the diffraction intensities. Data reduction was done with the ϕ (ρZ) method (Pouchou and Pichoir, 1984, 1985), and the resultant mean analysis for each grain is given in Table 5. H₂O values were obtained by calculation, taking into account the observed F values.

3. Discussion

There is a significant amount of work available in the literature on the structural aspects of richterites, and this is important in the context of the present study from a comparative point of view. Cameron and Gibbs (1971) refined the structures of two synthetic fluor-richterites (NaCaNaMg₅Si₈O₂₂F₂ and NaCaNaMg_{3.41}-Fe_{1.59}Si₈O₂₂F₂), and showed that Fe²⁺ strongly orders at the OH-free M(2) site. They argued that this preference is due to the well-known F-Fe²⁺ avoidance rule, which Rosenberg and Foit (1977) explained in terms of lower crystal field stabilization energy when F⁻ is the coordinated anion instead of OH⁻. Cameron *et al.* (1983) refined the structures of fluor-richterite and potassium-fluor-richterite at several temperatures. This end-member information is extremely useful when considering the detailed stereochemical behaviour of intermediate solid solutions. Oberti *et al.* (1992) characterized structures and site-occupancies of a large suite (12 samples) of richterites, and showed that in these amphiboles [4]-coordinated

Table 5. Electron microprobe analyses of richterites ; chemical formulae were calculated on the basis of 24 ($O^{2-} + F$).

	MR(1)	MR(2)	MR(3)	MR(4)
SiO ₂	54.81	55.10	54.69	55.49
Al ₂ O ₃	0.91	1.37	1.21	0.47
TiO ₂	0.01	0.01	0.01	0.03
FeO	2.00	1.87	1.64	1.63
MgO	20.00	19.95	20.37	18.35
MnO	6.57	6.72	6.32	7.83
CaO	4.92	4.92	5.73	5.94
Na ₂ O	5.75	5.66	5.43	5.26
K ₂ O	1.16	1.17	1.41	2.08
F	0.73	0.74	0.67	0.77
H ₂ O	(1.74)	(1.74)	(1.78)	(1.72)
O=F	-0.31	-0.31	-0.28	-0.32
Total	98.35	98.32	98.98	99.25
Chemical formulae:				
Si	7.880	7.918	7.816	7.997
Al	0.120	0.082	0.184	0.003
Sum T	8.000	8.000	8.000	8.000
Al	0.034	0.047	0.020	0.077
Ti	0.001	0.001	0.001	0.003
Fe	0.240	0.225	0.196	0.196
Mg	4.300	4.274	4.340	3.932
Mn	0.800	0.818	0.765	0.953
Sum C	5.375	5.365	5.322	5.161
C-5	0.375	0.365	0.322	0.161
Ca	0.758	0.757	0.877	0.915
Na	0.867	0.878	0.801	0.924
Sum B	2.000	2.000	2.000	2.000
Na	0.736	0.699	0.704	0.542
K	0.213	0.214	0.257	0.381
Sum A	0.949	0.913	0.961	0.923
F	0.332	0.336	0.303	0.350
OH	1.668	1.664	1.697	1.650

Ti⁴⁺ occurs at the T(2) site and [6]-coordinated Ti⁴⁺ at the M(1) site, the latter associated with partial O²⁻ for (OH,F)⁻ substitution at the O(3) site.

3.1 Comparison of the site occupancy refinement and electron microprobe results.

The scattering powers at the cation sites were refined unconstrained in the general refinement procedure. The resultant occupancy values provide the mean atomic number (which is equal to the number of neutral-atom electrons) at each site. Summing over all sites in each of the A-[A(2/m)+ 2 A(m)+ 2 A(2)], B- [2 M(4)+ 2 M(4')], and C- [2 M(1)+ 2 M(2)+ M(3)] groups of the standard chemical formula gives the corresponding values for these three groups. A totally independent assignment is provided by the

Table 6. Comparison of scattering powers at the A-, B- and C-group sites between the XRef results and the corresponding EMP analyses after conventional site assignment.

		MR(1)	MR(2)	MR(3)	MR(4)
A-group	XRef	11.4	12.0	12.3	12.7
	EMP	12.1	11.8	12.6	13.2
	Difference	-0.7	0.2	-0.3	-0.5
B-group	XRef	33.8	33.6	34.0	31.8
	EMP	34.1	33.9	34.4	32.5
	Difference	-0.3	-0.3	-0.4	-0.7
C-group	XRef	70.4	70.1	70.3	74.6
	EMP	69.7	69.1	68.5	73.1
	Difference	0.7	1.0	1.8	1.6
Total	XRef	115.6	115.7	116.6	119.2
	EMP	115.9	114.8	115.5	118.8
	Difference	-0.3	0.9	1.1	0.4

formula unit resulting from renormalization of the electron microprobe analyses. A comparison of these values is given in Table 6. The total numbers of electrons obtained from the two techniques for the analysed samples are in good agreement: the mean deviation is 0.5 electrons, which roughly corresponds to 0.5 % of the total observed m.a.n. ; however, the fact that those obtained from XRef are on the average slightly higher than those obtained by EMP may be worth further investigation. It should be noted here that the m.a.n.'s obtained by XRef have been intrinsically scaled by some internal standards, the m.a.n.'s at six oxygen sites being constrained to 8.0 and that at the T(2) site being constrained to 14.0. The mean deviations (XRef - EMP) for the three site groups are -0.32 (2.5 %), -0.42 (1.2 %) and 1.3 (1.9 %) electrons for the A-, B- and C-groups respectively. In terms of site occupancy, these differences correspond to less than 0.03 atoms per site when considering the most common substituents.

The data reported in Table 6 show a systematic difference suggesting that the cation assignments from the EMP data are not quite correct. The differences for the C-group are all positive, whereas the difference for the the B-group are all negative. The assignment was made assuming that the excess C-group cations entering the B-group sites were Mn²⁺ or Fe²⁺. The systematically positive and negative differences observed for these two groups suggest that some Mg may enter the B-group sites. Mg occupancies ≤ 0.05 a.p.f.u. would make the agreement extremely close.

3.2 The A-group sites

The K contents obtained from the EMP analyses can be used, together with the overall m.a.n.'s at these sites, to derive reasonable estimates for the Na contents at the A-group sites. They provide a good starting-point for the subsequent crystal-chemical considerations.

3.3 The B-group sites

As already discussed in Section 2.2, a peak of residual electron density near the M(4) site in the difference Fourier maps indicates the presence of cations other than Ca and Na which, as discussed in Section 3.1, could be Mn^{2+} , Fe^{2+} and/or Mg. These smaller cations will not occupy the same position as Ca and Na in the M(4) cavity, as their size and bonding characteristics are significantly different from those of Ca and Na. Table 7 reports the M(4) coordination geometry for cummingtonite (Fisher, 1966), manganooan cummingtonite (Papike *et al.*, 1969) and grunerite (Finger, 1969) respectively, and compares them with that of fluor-richterite (Cameron *et al.*, 1983) and with the M(4) and M(4') coordination geometries obtained in this work for the sample with the highest m.a.n. at the M(4') position, *i.e.* MR(2); the geometrical data published more recently by Ghose and Hexiong (1989) for a manganooan cummingtonite with 1.67 Mn^{2+} a.p.f.u. at M(4) are nearly identical to those reported by Papike *et al.* (1969) and are not listed in Table 7. The correspondence of the local geometry and of the γ coordinate of M(4) with respect to F-richterite and of M(4') with respect to Fe-Mg-Mn-amphiboles is immediately apparent, and confirms that the solid solution of a Fe-Mg-Mn component in those Ca-Na-amphiboles reflects into the occurrence of the M(4') site.

The next issue is related to the details of the occupancy of B-group cations. Given the good agreement between the XRef and EMP results, the aggregate m.a.n. resulting at the B- group

Table 7. Stereochemistry about the M(4) site in Fe-Mg-Mn-amphiboles and in richterites.

	1	2	3	4	MR(2) M(4)	MR(2) M(4')
cat-0(2)	2.164	2.204	2.135	2.421	2.391	2.150
-0(4)	2.023	2.109	1.988	2.339	2.310	2.275
-0(5)	3.143	3.101	3.298	2.884	2.880	3.076
-0(6)	2.691	2.592	2.757	2.571	2.612	2.855
<cat-0> [8]	2.505	2.502	2.545	2.544	2.548	2.589
<cat-0> [6]	2.293	2.302	2.293	2.444	2.438	2.427
γ coord.	0.2597	0.2636	0.2574	0.2757	0.2752	0.2578

1 = cummingtonite (Fisher, 1966) ; 2 = manganooan cummingtonite (Papike *et al.*, 1969) ; 3 = grunerite (Finger, 1969) ; 4 = F-richterite (Cameron *et al.*, 1983).

sites from XRef can be used, together with the Ca and the residual Na [$N_{\text{A tot}} - Na(A)$] occupancies obtained from the EMP analyses, to derive reliable occupancies for (Mn^{2+} , Fe^{2+} , Mg). If we calculate the m.a.n. attributable to the (Mn^{2+} , Fe^{2+} , Mg) mixture, which is equal to m.a.n.(B) - [20 Ca(B) + 11 Na(B)], and divide it by the residual B-occupancy (1-Ca-Na), we obtain a m.a.n. for (Mn^{2+} , Fe^{2+} , Mg) lower than 25 electrons. Because the analysis of the EMP data (Section 3.1) has shown that the Mg(B) content should not exceed 0.05 a.p.f.u., this result indicates that Mn^{2+} is the most abundant substituent, and that no Fe^{2+} is present at the B- group sites (see the final site populations reported in Table 8).

In conclusion, Mn^{2+} in richterites is strongly ordered at the B-group sites with respect to Fe^{2+} . A further confirmation of the low B-site preference of Fe^{2+} in richterites comes from comparison with the structure refinements of Oberti *et al.* (1992) for Mn-poor richterites (Mn^{2+} never exceeding 0.10 a.p.f.u., Fe^{2+} between 0.0 and 0.58 a.p.f.u.). In that case, the M(4') splitting was observed (and refined giving < 0.5 electrons p.f.u.) only when the total Fe^{2+} exceeded 0.5 a.p.f.u. Other supporting evidence for the Mn B-site preference could be gained by a Mössbauer study of these manganooan richterites.

Table 8. Site-group assignments according to EMP and XRef results.

Sample	A-group				B-group				C-group				T-group		O(3)					
	Na	K	e(o)	e(c)	Na	Mg	Ca	Mn^{2+}	e(o)	e(c)	Mg	Al	Mn^{2+}	Fe^{2+}	e(o)	e(c)	Si	Al	OH ⁻	F ⁻
MR(1)	0.68	0.21	11.5	11.5	0.89	-	0.76	0.34	33.8	33.5	4.22	0.08	0.46	0.24	70.4	69.4	7.92	0.08	1.67	0.33
MR(2)	0.74	0.20	12.0	11.9	0.88	0.02	0.75	0.35	33.6	33.6	4.26	0.04	0.46	0.24	70.1	69.4	7.90	0.10	1.66	0.34
MR(3)	0.69	0.24	12.3	12.4	0.81	0.02	0.88	0.29	34.0	34.0	4.26	0.04	0.46	0.24	70.3	69.4	7.84	0.16	1.70	0.30
MR(4)	0.55	0.35	12.7	12.7	0.90	0.05	0.92	0.13	32.0	32.1	3.92	0.06	0.82	0.20	74.6	73.5	7.94	0.06	1.65	0.35

3.3 The T-group sites

The stereochemical details of the tetrahedra are conformable with previous findings (Oberti *et al.*, 1992) and with the chemistry of these richterites (Table 5). The observed $\langle T(1)-O \rangle$ distances are those expected from the small amounts of $[^4]Al^{3+}$ estimated by EMP. The observed $\langle T(2)-O \rangle$ distances confirm complete $[^4]Si^{4+}$ occupancy at the T(2) site.

3.4 The C-group cations

Stereochemical details of the octahedral coordination polyhedra are given in Table 3, and the cation contents assigned to the C-group from the EMP analyses are given in Table 5. There is no significant Ti in any of these amphiboles, thus we are not concerned with the possibility of $[^6]Ti^{4+}$ at M(1) combined with the presence of O^{2-} at O(3). The $[^6]Al^{3+}$ contents are small, and extensive previous work on amphiboles indicates that it is ordered at the M(2) site. Thus the primary problem is to consider the distribution of Mg, Mn and Fe over the M(1), M(2) and M(3) sites. The presence of significant Mn^{3+} and Fe^{3+} contents can be discounted for the following reasons: (1) the long $\langle M(2)-O \rangle$ distances observed in all the samples are not compatible with the presence of small cations at M(2); (2) the good agreement in terms of overall m.a.n.'s between the XRef and EMP results when the latter are recalculated with all Fe as FeO and all Mn as MnO; (3) the difficulties in balancing the extra positive charge that would result from the presence of highly charged octahedral cations. This could be done either by lowering the Na content at the A- and B-group sites or by increasing the $[^4]Al^{3+}$ contents; Na contents from EMP may sometimes be underestimated, but are very rarely overestimated, and the second hypothesis can be rejected when taking into account the observed $\langle T(1)-O \rangle$ distances.

With the further constraint that the overall chemical formulae must be neutral, reasonable site-group assignments can now be obtained (see Table 8) from XRef and EMP results.

Concerning the distribution of Mg, Mn^{2+} and Fe^{2+} among the three independent sites, it must be noted that Mn^{2+} has by far the largest cation-oxygen distance of the usual octahedral cations: for clinopyroxenes, $\langle Mn^{2+}-O \rangle = 2.173 \text{ \AA}$ in johannsenite ($CaMn^{2+}Si_2O_6$, Freed and Peacor, 1967), whereas $\langle Fe^{2+}-O \rangle = 2.130 \text{ \AA}$ in hedenber-

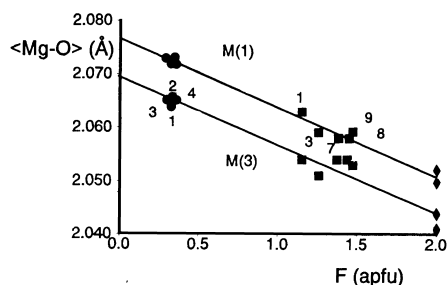


Fig. 1. Variations in $\langle Mg-O \rangle$ distances at M(1) and M(3) as a function of F^- content at O(3). Circles = this work; squares = $[^6]Ti^{4+}$ -free Mn-poor F-richterites from Oberti *et al.* (1992), numbering is the same as in the original paper; diamonds = F- and K-F-richterites from Cameron *et al.* (1983).

gite ($CaFe^{2+}Si_2O_6$, Cameron *et al.*, 1973). In contrast to most amphibole end-members, in richterites the M(2) octahedron is larger than the M(1) and M(3) octahedra (Oberti *et al.*, 1992). The hypothesis that Mn^{2+} orders at M(2) and does not distribute over the M(1) and M(3) sites seems therefore reasonable. Moreover, the presence of significant F^- substitution after OH- provokes a further contraction of the m.b.l.'s at the two octahedral sites coordinating O(3), *i.e.* M(1) and M(3).

Fig. 1 shows $\langle M(1)-O \rangle$ and $\langle M(3)-O \rangle$ in richterite vs. F^- content in a.p.f.u. from the EMP (circles are the samples of this work, squares are the $[^6]Ti^{4+}$ -free F-richterites of Oberti *et al.* (1992), diamonds are synthetic F-richterites ($F^- = 2$ a.p.f.u.) from Cameron *et al.*, 1983). Also Fe^{2+} substitution for Mg affects octahedral size: $\langle Fe^{2+}-O \rangle = 2.120$ and $\langle Mg-O \rangle = 2.078 \text{ \AA}$ are the values actually used in the CORANF procedure, which has been designed to obtain the octahedral site populations in amphiboles (Ungaretti *et al.*, 1983; Cannillo *et al.*, 1986). The values reported for $\langle M(1)-O \rangle$ and $\langle M(3)-O \rangle$ have therefore been normalized to complete Mg occupancy. As the overall m.a.n.'s from XRef are always slightly higher than those obtained from EMP analysis, these are to be considered the maximum Fe^{2+} contents for those samples. The two linear regression equations [$\langle Mg-O \rangle_{M(1)}$ (Å) = $2.0769 - 0.0130 F^-$ (a.p.f.u.); $\langle Mg-O \rangle_{M(3)}$ (Å) = $2.0696 - 0.0128 F^-$ (a.p.f.u.)] have r values equal to -0.994 and -0.978 respectively. The similar $[4 O^{2-} + 2 (OH,F)^-]$ coordination of the two sites justifies the two trends being practically parallel; the fact that the two $(OH,F)^-$ are in a *cis*

Table 9. Octahedral site populations obtained after the crystal-chemical analysis of the experimental data.

Sample	M(1)				M(2)						M(3)			
	Mg	Fe ²⁺	d(o)	d(c)	Mg	Al	Mn ²⁺	Fe ²⁺	d(o)	d(c)	Mg	Fe ²⁺	d(o)	d(c)
MR(1)	0.95	0.05	2.074	2.075	0.67	0.04	0.23	0.06	2.096	2.096	0.98	0.02	2.065	2.067
MR(2)	0.96	0.04	2.075	2.075	0.68	0.02	0.23	0.07	2.097	2.099	0.98	0.02	2.067	2.067
MR(3)	0.95	0.05	2.075	2.075	0.69	0.02	0.23	0.06	2.097	2.098	0.98	0.02	2.066	2.067
MR(4)	0.93	0.07	2.075	2.076	0.54	0.03	0.41	0.02	2.111	2.112	0.98	0.02	2.066	2.067

Observed m.b.l.'s have been obtained as described in the text.

arrangement at M(1) but in a *trans* arrangement at M(3) does not in this case affect the m.b.l. dependence vs. F⁻ in different ways

The octahedral site populations listed in Table 9 were obtained by distributing the C-group site-occupancies reported in Table 8 according to the observed m.a.n.'s and m.b.l.'s obtained from XRef subject to the following crystal-chemical constraints : (1) full occupancy of the sites ; (2) overall neutrality of the formula ; (3) observed m.a.n.'s as linear combinations of the atomic numbers of each single constituent multiplied by its site occupancy ; (4) observed m.b.l.'s as linear combinations of each single <cation-O> distance at that site multiplied by the site occupancy. In the case of the M(2) site, the values reported in Hawthorne *et al.* (1993) were used : <Mg-O> = 2.078, <Al-O> = 1.925, <Mn²⁺-O> = 2.170, <Fe²⁺-O> = 2.120 (Å). In the case of the M(1) and M(3) sites, <Mg-O> = 2.073 and 2.066 Å respectively were obtained from Fig. 1 for F⁻ = 0.33 a.p.f.u. ; <Fe²⁺-O> = 2.115 and 2.108 Å respectively were obtained by adding to the latter the difference 2.120 - 2.078 = 0.042 Å.

The small deviations between observed and calculated m.b.l.'s in Table 9 support the hypothesis of Mn²⁺ ordering at M(2). The fairly regular Fe²⁺ distribution over the octahedral sites may be attributed to the need for dimensional matching of the three independent M(1), M(2) and M(3) sites in the octahedral strip. The same kind of reasoning also suggests that significantly higher F contents (which are common in richterite) may be inhibited by high Mn²⁺ contents at M(2). This hypothesis should be checked with Mn-rich richterites from other localities. Unfortunately, as far as we know the only other reported analysis of such composition is from a "tirodite" host-lamella pair from Tirodi mine, Madhya Pradesh, India (analysis n. 3 in Ghose *et al.*, 1974). Apart from the difficulties in obtaining reliable analyses in that situation, no F analysis is reported for this amphibole.

4. Conclusions

Site-occupancy refinement and stereochemical analysis for low-Fe manganian richterites show that Mn²⁺ behaves in the following manner in these amphiboles :

- (1) there is significant occupancy at the B-group sites by Mn²⁺, which enters a position displaced towards the octahedral strip relative to the M(4) site ; the latter is occupied only by Ca and Na. This split M(4') position has coordination very similar to that observed in Fe-Mg-Mn-amphiboles.
- (2) at the octahedral C-group sites, Mn²⁺ shows a very strong preference for the M(2) site ;
- (3) the increase in the <M(2)-O> distance due to Mn²⁺ substitution prevents high-charged octahedral cations from entering the richterite structure in significant amounts ; because of the need for dimensional matching among the octahedra, one could also infer that high Mn²⁺ contents inhibit extensive F⁻ ⇌ OH⁻ substitution (which is the norm in Mn-free or Mn-poor richterite).

Acknowledgements : Prof. Mirella Bondi (University of Bologna, Italy) kindly provided one of the rock-sample used for this study. Financial assistance was provided by CNR-NATO and the Natural Sciences and Engineering Research Council of Canada.

References

- Bacon, G.E. (1969) : Coherent neutron-scattering amplitudes. *Acta Cryst.*, **A25**, 391-392.
- Cameron, M., Gibbs, G.V. (1971) : Refinement of the crystal structure of two synthetic fluor-rich richterites. *Carnegie Inst. Wash. Year Book*, **70**, 150-153.
- Cameron, M., Sueno, S., Prewitt, C.T., Papike, J.J. (1973) : High-temperature crystal-chemistry of acmite, diopside, hedenbergite, jadeite, spodumene and ureyite. *Am. Mineral.*, **58**, 594-618.

- Cameron, M., Sueno, S., Papike, J.J., Prewitt, C.T. (1983) : High temperature crystal-chemistry of K and Na fluor-richterites. *Am. Mineral.*, **68**, 924-943.
- Cannillo, E., Ungaretti, L., Oberti, R., Smith, D.C. (1986) : An updated version of computer program CORANF for obtaining the site populations and the bulk-mineral compositions of *C2/m* amphiboles by single crystal X-ray diffractometry and refinement. Proceedings of the XIV International Mineralogical Association Meeting, Stanford, 70.
- Finger, L.W. (1969) : The crystal structure and cation distribution of a grunerite. *Mineral. Soc. Spe. Pap.*, **2**, 95-100.
- Fisher, K.F. (1966) : A further refinement of the crystal structure of cummingtonite, $(\text{Mg,Fe})_7(\text{Si}_4\text{O}_{11})_2(\text{OH})_2$. *Am. Mineral.*, **51**, 814-818.
- Freed, R.L., Peacor, D.R. (1967) : Refinement of the crystal structure of johannesite. *Am. Mineral.*, **52**, 709-720.
- Ghose, S., Forbes, W.C., Phakey, P.P. (1974) : Unmixing of an alkali amphibole (tirodite) into magnesio-richterite and magnesio-riebeckite. *Indian J. Earth Sci.*, **1**, 37-42.
- Ghose, S., Hexiong, Y. (1989) : Mn-Mg distribution in a *C2/m* manganian cummingtonite : crystal-chemical considerations. *Am. Mineral.*, **74**, 1091-1096.
- Ghose, S., Kersten, M., Langer, K., Rossi, G., Ungaretti, L. (1986) : Crystal field spectra and Jahn Teller effect of Mn^{3+} in clinopyroxenes and clinoamphiboles from India. *Phys. Chem. Minerals*, **13**, 291-305.
- Hawthorne, F.C. (1983a) : Quantitative characterization of site- occupancies in minerals. *Am. Mineral.*, **68**, 287-306.
- (1983b) : The crystal chemistry of amphiboles. *Can. Mineral.*, **21**, 173-480.
- Hawthorne, F.C., Ungaretti, L., Oberti, R., and Bottazzi, P. (1993) : Li : an important component in igneous alkali amphiboles. *Am. Mineral.*, submitted.
- Lehman, M.S., Larsen, F.K. (1974) : A method for location of the peaks in step-scan-measured Bragg reflections. *Acta Cryst.*, **A30**, 580-586.
- North, A.C.T., Phillips, D.C., Mathews, F.S. (1968) : A semi-empirical method of absorption correction. *Acta Cryst.*, **A24**, 351-359.
- Oberti, R., Ungaretti, L., Cannillo, E., Hawthorne, F.C. (1992) : The behaviour of Ti in amphiboles: I. Four- and six-coordinated Ti in richterites. *Eur. J. Mineral.*, **4**, 425-439.
- Papike, J.J., Ross, M., Clark, J.R. (1969) : Crystal-chemical characterization of clinoamphiboles based on five new structure refinements. *Mineral. Soc. Amer. Spec. Pap.*, **2**, 117-136.
- Pouchou, J.L., Pichoir, F. (1984) : A new model for quantitative analysis: Part I. Application to the analysis of homogeneous samples. *La recher. Aerosp.*, **5**, 47-65.
- Pouchou, J.L., Pichoir, F. (1985) : 'PAP' $\phi(\rho Z)$ procedure for improved quantitative microanalysis. *Micr. Anal.*, 1985, 104-106.
- Rosenberg, P.E., Foit, F.F. (1977) : Fe^{2+} -F avoidance in silicates. *Geochim. Cosmochim. Acta*, **41**, 345-346.
- Rossi, G., Oberti, R., Dal Negro, A., Molin, G.M., Melini, M. (1987) : Residual electron density at the M2 site in *C/2c* clinopyroxenes: relationships with bulk chemistry and sub-solidus evolution. *Phys. Chem. Minerals*, **14**, 514-520.
- Ungaretti, L. (1980) : Recent developments in X-ray single crystal diffractometry applied to the crystal-chemical study of amphiboles. *God. Jugo. Cen. Kristalograf.*, **15**, 29-65.
- Ungaretti, L., Smith, D.C., Rossi, G. (1981) : Crystal-chemistry by X-ray structure refinement and electron microprobe analysis of a series of sodic-calcic to alkali amphiboles from the Nybø eclogite pod. *Bull. Minéral.*, **104**, 400-412.
- Ungaretti, L., Lombardo, B., Domeneghetti, C., Rossi, G. (1983) : Crystal-chemical evolution of amphiboles from eclogitised rocks of the Sesia Lanzo Zone, Italian Western Alps. *Bull. Minéral.*, **106**, 645-672.

Received 4 April 1992

Accepted 31 August 1992

